Scanning tunneling microscopy of Bi-induced Ag(111) surface structures

Chiaki Kato, Yuki Aoki, and Hiroyuki Hirayama*
Department of Materials Science and Engineering, Tokyo Institute of Technology, J1-3, 4259 Nagatsuda, Midori-ku, Yokohama 226-8502, Japan

(Received 28 June 2010; revised manuscript received 3 September 2010; published 5 October 2010)

Submonolayer Bi-induced structures at the surfaces of 20-monolayer (ML)-thick Ag(111) films on Si(111)7×7 substrates were investigated using scanning tunneling microscopy. Bi atoms initially adsorbed randomly in the region of Bi coverage (θ_{Bi}) below 1/3 ML. However, local $\sqrt{3}\times\sqrt{3}$ ordering was extended with increasing θ_{Bi} and $\sqrt{3}\times\sqrt{3}$ reconstruction was completed at $\theta_{Bi}=1/3$ ML. At larger θ_{Bi}, the surface was covered with a striped structure. Bi atoms were arranged with centered rectangular unit cells, although the contrast of the cell changed periodically along the $\{01\bar{1}\}$ direction. As a result, bright and dark stripes along the $\{\bar{2}11\}$ direction appeared alternatively at the surfaces. A close-packed Bi-induced $\begin{pmatrix}3 & 0\\ 1 & 2\end{pmatrix}$ structure is proposed as a model for the striped surface structure.

DOI: 10.1103/PhysRevB.82.165407 PACS number(s): 68.35.bd, 68.37.Ef, 68.43.Fg

I. INTRODUCTION

A 1/3 Bi monolayer (ML) induces a $\sqrt{3}\times\sqrt{3}$ reconstruction at the Ag(111) surface. The Bi/Ag(111)$\sqrt{3}\times\sqrt{3}$ surface reconstruction has received considerable attention recently, because it gives rise to giant spin splitting of the surface state.[1–7] In principle, the Kramers degeneracy of electronic bands are spontaneously lifted at surfaces due to breaking of the spatial inversion symmetry of the bulk crystal.[8] The splitting is further enhanced by the presence of heavy atoms at the surface due to Rashba-Vicikov-type spin-orbit interactions.[9] Because Bi has a high atomic number ($Z=83$), it is reasonable that a large spin-splitting effect is observed for the Bi-induced $\sqrt{3}\times\sqrt{3}$ surface.

However, the magnitude of the spin splitting at the Bi/Ag(111)$\sqrt{3}\times\sqrt{3}$ surface is extremely large compared with that at pure metal surfaces.[10–17] Angle-resolved photoelectron spectroscopy studies have shown that the splitting of the surface state in k space (Δk) is 0.004 Å^{-1} for Ag(111) ($Z=47$),[1] 0.012–0.014 Å^{-1} for Au(111) ($Z=79$),[10–12] and 0.05 Å^{-1} for Bi(111) surfaces ($Z=83$).[16] The splitting increases with Z, as expected based on the Z-dependent enhancement of the spin-orbit interaction. Considering this trend, spin splitting at a Bi/Ag(111) surface with θ_{Bi}(Bi coverage)=1/3 ML is expected to be smaller than that at a Bi(111) surface with $\theta_{Bi}=1$ ML. However, the Bi/Ag(111)$\sqrt{3}\times\sqrt{3}$ surface exhibits a giant spin splitting of 0.13 Å^{-1},[1] which is much larger than that predicted by the normal Z dependence for pure metallic surfaces.

Distortion of the surface-state wave function and the in-plane gradient of the surface electronic potential have been theoretically identified as causes of the giant spin splitting.[1,6,7,13,18] Although Bi and Ag are immiscible in bulk form, the Bi atoms assume substitutional sites and form an alloy layer at the Bi/Ag(111)$\sqrt{3}\times\sqrt{3}$ surface. However, the substitutional Bi atoms buckle outward from the surface, because their atomic radius is larger than that of the Ag atoms.[6] This specific atomic arrangement induces distortion of the wave function[6] and breaks the in-plane inversion symmetry at the surface.[1,7]

Apart from the Bi/Ag(111) system, Pb($Z=82$) and Sb($Z=51$) are also known to be immiscible in the bulk, but form $\sqrt{3}\times\sqrt{3}$-reconstructed surface alloys on Ag(111) (Refs. 18–23) and Cu(111) surfaces.[24] Bi atoms at the Cu(111) surface also form a $\sqrt{3}\times\sqrt{3}$-reconstructed surface alloy.[25,26] However, $\sqrt{3}\times\sqrt{3}$-reconstructed surface alloys other than that in the Bi/Ag(111) system have been found to exhibit only a small spin splitting of the surface state.[3,6,18,23,24,27] Thus, the giant spin splitting is thought to be specific to the Bi-induced $\sqrt{3}\times\sqrt{3}$ reconstruction at the Ag(111) surface.

However, a two-photon photoemission study[28] reported very recently that two unoccupied surface states of the Bi-induced $\begin{pmatrix}2 & 0\\ 1 & 2\end{pmatrix}$ [hereafter, referred to as (2012)] reconstruction at the Cu(111) surface exhibits spin splitting as large as that for the Bi/Ag(111)$\sqrt{3}\times\sqrt{3}$ reconstruction, although the Bi/Cu(111)$\sqrt{3}\times\sqrt{3}$ surface exhibits a very small spin splitting of $\Delta k=0.03$ Å^{-1}.[24] At the Cu(111) surface, the $\sqrt{3}\times\sqrt{3}$ surface alloy with $\theta_{Bi}=1/3$ ML changes to the (2012) dealloyed reconstruction at $\theta_{Bi}\geq 0.45$ ML.[25,26] Considering the similarity between the Ag and Cu(111) surfaces, it is expected that the Ag(111) surface would also assume a new (2012)-like surface reconstruction with a spin splitting even larger than that at the Bi/Ag(111)$\sqrt{3}\times\sqrt{3}$ surface with $\theta_{Bi}\geq 1/3$ ML. To reveal the essential origin of the giant spin splitting at the Bi/Ag(111)$\sqrt{3}\times\sqrt{3}$ and Bi/Cu(111) (2012) surfaces, a comparative study on the structure and spin splitting, and theoretical band calculations based on the experimentally determined surface structure is highly desirable for high θ_{Bi} phases at Ag(111) surfaces. However, to the best of our knowledge, no reconstruction other than the $\sqrt{3}\times\sqrt{3}$ with $\theta_{Bi}=1/3$ ML has been investigated in the Bi/Ag(111) system.

In this study, we investigate the θ_{Bi}-dependent change in the reconstruction at the (111) surface of 20-ML-thick Ag epitaxial films on Si(111)7×7 substrates. In addition to the (111) surface of bulk Ag, the deposition of 1/3 ML Bi atoms has been previously reported to give rise to the $\sqrt{3}\times\sqrt{3}$ reconstruction with giant surface-state spin splitting around $\bar{\Gamma}$ at the surfaces of 11–22-ML-thick ultrathin Ag(111) epitaxial films on Si substrates.[4,5] The spin-split band surface state hybridizes with the quantum well states of the Ag films at k away from the $\bar{\Gamma}$ point. However, it is considered that the

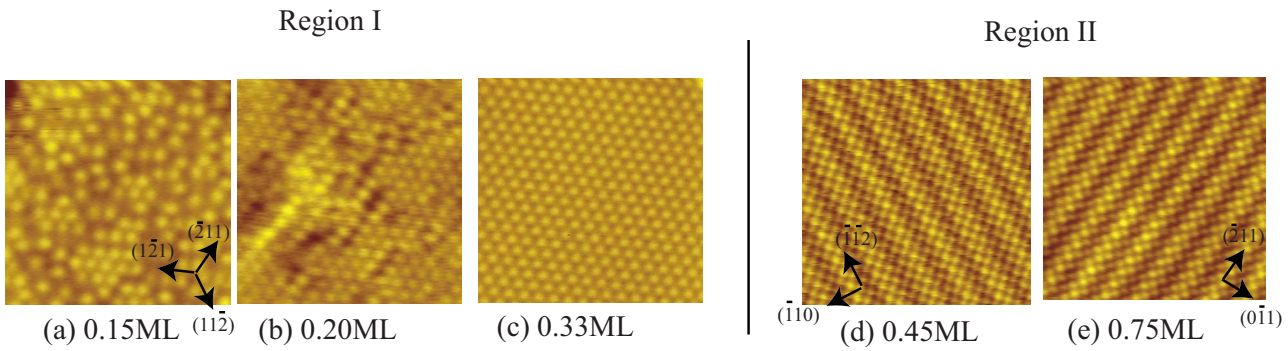

FIG. 1. (Color online) STM images of Bi-induced Ag(111) surfaces for (a) 0.15, (b) 0.20, (c) 0.33, (d) 0.45, and (e) 0.75 ML. The image size is 7.5×7.5 nm^2 . The imaging conditions were $V_s=+0.6$ V, $I_t=0.1$ nA for (a)–(c) and $V_s=+0.2$ V, $I_t=0.1$ nA for (d) and (e). The temperature was 68 K.

ultrathin Ag(111) epitaxial films exhibit the same surface reconstruction features as bulk Ag(111). In addition, it introduces the possibility of introducing spin band splitting into the realm of silicon technology.[5] Therefore, we systematically investigated the change in the reconstruction with θ_{Bi} on 20-ML-thick Ag(111) film surfaces using scanning tunneling microscopy (STM).

II. EXPERIMENT

The investigation was carried out in an ultrahigh-vacuum (UHV) apparatus equipped with a cryogenic sample cooling system, Ag and Bi Knudsen cells, a reflection high-energy electron-diffraction system, and a low-temperature STM unit.[29,30] The Ag(111) surfaces were prepared by depositing Ag on *n*-type Si(111) substrates. Prior to Ag deposition, the Si(111) substrates were preheated at 900 K overnight and then cleaned by flashing at 1400 K for 10 s under UHV. The cleanliness of the substrates was confirmed by observing a defect-free 7×7 reconstruction by STM. 20-ML-thick Ag films were deposited on the clean substrates at 100 K and then slowly annealed to 300 K overnight. This two-step process resulted in the epitaxial growth of Ag(111) films with a very flat morphology.[31,32] Submonolayer Bi films were then deposited on the flat Ag(111) film surfaces at a rate of 0.012 ML/s. θ_{Bi} was defined with respect to the surface atom density at the Ag(111) surface. The deposition temperature was set at 370–460 K to obtain well-ordered surface alloy structures[20,21,25] and was monitored using an optical pyrometer.

The Bi-adsorbed Ag(111) surface structures were observed using STM with a bias voltage applied to the samples. Electrochemically etched polycrystalline W was used for the STM tips. The tips were cleaned by electron bombardment in the UHV apparatus prior to STM measurement. STM images were taken at 68 K with a supercooled liquid N_2 cryostat attached to the STM unit. Some images were also taken at room temperature (RT). The image size was calibrated with respect to the 7×7 unit cell of the Si(111) clean surfaces. The crystallographic directions at the Ag(111) surface were determined with respect to the unit cell of the Si(111)7×7 substrates because the Ag films were epitaxially grown on the Si substrates. 7×7 unit cells with faulted and unfaulted half unit cells were used to determine the $\{\bar{2}11\}$ and $\{01\bar{1}\}$ directions.

III. RESULTS AND DISCUSSION

The θ_{Bi}-dependent change in the STM images is summarized in Fig. 1. The $\sqrt{3}\times\sqrt{3}$ reconstruction was observed to evolve in the coverage region $0<\theta_{\mathrm{Bi}}<1/3$ ML (region I) and was completed at $\theta_{\mathrm{Bi}}=1/3$ ML. A striped structure then appeared at larger coverages (region II). The striped structure showed three rotationally equivalent domains in the large-scale images (not shown) due to the threefold rotational symmetry of the Ag(111) surface. The stripes extended along one of the three equivalent $\{\bar{2}11\}$ directions in each domain, as shown in Figs. 1(d) and 1(e). In both regions I and II, no differences in the surface structures were found in the STM images taken at 68 K and at RT. Detailed results and a separate discussion of regions I and II are given in the following.

A. Region I: $0<\theta_{\mathrm{Bi}}\leq1/3$ ML

In this region, a small number of protrusions appeared randomly at a low coverage $\theta_{\mathrm{Bi}}=0.15$ ML [Fig. 1(a)]. However, the arrangement of the protrusions exhibited hexagonal ordering as θ_{Bi} increased [Fig. 1(b)]. The protrusions were ~0.02 nm in height. The position of the protrusions did not change in either the positively (i.e., empty state) or negatively biased (i.e., occupied state) STM images, which suggests that they mainly reflect topographic corrugations. In addition, the number of protrusions increased with θ_{Bi}; therefore, the protrusions are assigned as Bi atoms.

A full hexagonal array of Bi atoms was formed at $\theta_{\mathrm{Bi}}=0.33$ ML [Fig. 1(c)]. The Bi-Bi atom distance was 0.48 nm, which is very close to $\sqrt{3}\times\alpha=0.50$ nm [$\alpha=0.29$ nm; the 1×1 unit cell length of the Ag(111) surface lattice]. Furthermore, the Bi atoms were confirmed to align along the $\{\bar{2}11\}$ direction. Thus, the hexagonal array is unambiguously assigned as the Bi-induced $\sqrt{3}\times\sqrt{3}$-$R30°$ reconstruction at the Ag(111) surface. Figure 1(c) is consistent with the previous STM image of the Bi/Ag(111)$\sqrt{3}\times\sqrt{3}$ surface at $\theta_{\mathrm{Bi}}=1/3$ ML, in which protrusions were reported to form a hexagonal array with a distance of 0.5 nm.[2]

Bi atoms have been reported to occupy substitutional sites and form a surface alloy phase for the Bi-induced $\sqrt{3}\times\sqrt{3}$ reconstruction at the bulk crystalline Ag(111) surface.[1,2,6,7,18] The Ag(111) surface is under tensile stress so that incorporation of larger atoms in the top surface layer reduces the tensile stress and consequently the surface energy; thus, Bi atoms favor substitutional sites at the Ag(111) surface in order to reduce surface tension,[25] although the larger Bi atoms (r_{Bi}=0.163 nm) cannot be fully incorporated into the closely packed (111) surface of smaller Ag atoms (r_{Ag}=0.144 nm) and are pushed slightly outward.[6] In this respect, we consider that the Bi atoms assume substitutional sites in the initial stage of adsorption, even before completion of the $\sqrt{3}\times\sqrt{3}$ reconstruction.

It would be expected that the tensile stress at the ultrathin Ag film surface is stronger than that at the bulk Ag(111) surface because Si has a larger lattice constant than Ag. However, several studies on the Ag film thickness-dependent shift in Shockley-type surface states revealed that misfit-induced lattice distortion is less than 1% in this system.[29,30,33] Thus, the surface of the ultrathin Ag film is considered to exhibit the same stress-induced preference for substitutional sites for Bi atoms to that at the bulk crystalline Ag(111) surface.

Detailed inspection reveals that the Bi atoms are arranged locally with $\sqrt{3}$ ordering in several regions, even for such a small θ_{Bi} as 0.15 ML [for example, at the lower middle area in Fig. 1(a)]. This indicates that Bi-Bi interaction occurs, which prefers $\sqrt{3}\times\sqrt{3}$ local ordering, although the interaction is not sufficiently strong to separate the surface completely into two phases of Bi-induced $\sqrt{3}$ local domains and a Bi-free region at small θ_{Bi}.

The local $\sqrt{3}$ ordering is considered to be due to the balance between the attractive and repulsive interactions of Bi atoms at the surface. The surface-state-medicated spatial modulation of the adsorption potential has been suggested as a cause of the attractive interaction for low coverages of Cs adatoms on the Ag(111) surface.[34,35] For low Cs coverage, the Ag surface-state electrons are scattered by Cs adatoms giving rise to Friedel oscillation of the surface electron density around the Cs adatoms. The adsorption potential for Cs is lowered at the local maxima in the oscillation; therefore, the Ag surface state mediates the attractive interaction between Cs adatoms. Simultaneously, the Cs adatoms undergo a repulsive interaction due to the dipole-dipole interaction between them. The balance between the surface-state-mediated and dipole-dipole interactions was reported to produce hexagonal ordered phases in very low temperature ($T \leq 7$ K) STM studies.[34,35] A similar scenario could hold for the Bi/Ag(111) system, although the dipole interaction between Bi atoms would be weaker than that between Cs atoms with lower ionization energy. However, the surface-state-mediated attractive potential is on the order of 1 meV.[34,35] The STM observations were carried out at T=68 K($\simeq$6 meV); the surface-state-mediated attractive interaction is too small to suppress the thermal diffusion of surface atoms under the experimental conditions. Thus, the balance between the surface-state-mediated and dipole-dipole interactions is not the cause of the local $\sqrt{3}$ ordering preference in this case. Alternatively, we suppose that the substitutional Bi-induced lowering of the electronic energy and strain effects play roles in the weak preference for local $\sqrt{3}$ ordering, although the detailed mechanism is not clear at present.

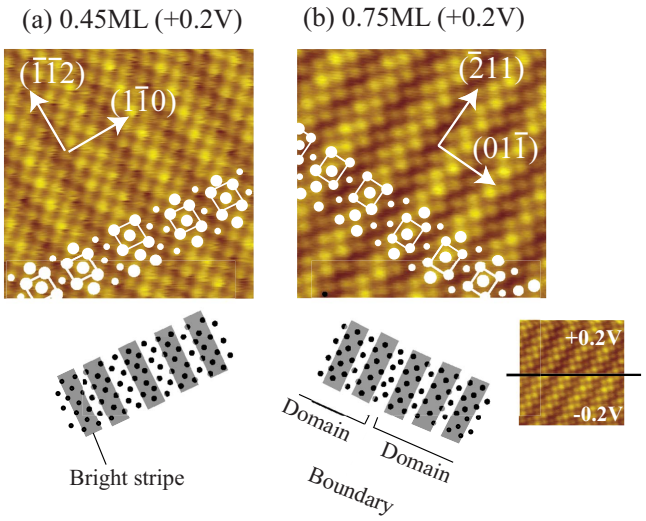

FIG. 2. (Color online) High-resolution STM images of the (a) θ_{Bi}=0.45 ML and (b) 0.75 ML surfaces. The imaging size is 5.2 nm^2. The images were taken at 68 K with V_s=+0.20 V, I_t=0.1 nA. The position of the protrusions is indicated by white dots. The size of the dot represents the brightness at that position. Fundamentally, the protrusions aligned with a centered rectangular cell (indicated by the white lines) with a size of 0.40 ± 0.01 nm in the $\{01\bar{1}\}$ direction and 0.49 ± 0.01 nm in the $\{\bar{2}11\}$ direction. The alternating contrast of the protrusions along the $\{01\bar{1}\}$ direction causes extension of the stripes in the $\{\bar{2}11\}$ direction. The relationship between the protrusions and the bright and dark stripes is illustrated below the STM images, where the bright stripes are indicated by gray lines. The small STM image in the lower right side shows the bias-polarity dependence of the stripe structure at θ_{Bi}=0.75 ML. The image was independent of the change in bias voltage from +0.2 to −0.2 V during the scan.

B. Region II: $\theta_{Bi} \geq 1/3$ ML

At $\theta_{Bi} \geq 1/3$ ML, the $\sqrt{3}\times\sqrt{3}$ reconstruction changed to the striped structure. The range of θ_{Bi} corresponding to the transition region from the $\sqrt{3}\times\sqrt{3}$ to the striped structure could not be determined exactly. However, the surface was completely changed to the striped structure, at least at $\theta_{Bi} \geq 0.45$ ML [Fig. 1(d)]. At larger θ_{Bi}, the surface always exhibited the striped structure in region II.

High-resolution STM images of the striped structure at θ_{Bi}=0.45 ML and 0.75 ML are depicted in Figs. 2(a) and 2(b), respectively. Such atomically resolved STM images were difficult to obtain for the striped structures. Frequently, neighboring atoms could not be resolved and were imaged as short slanted bars or twigs in the stripes. The contrast of the stripes was missing in some cases. However, the appearance of the slanted bars and twigs was not reproducible and had no specific voltage or polarity dependence. High-resolution STM images of the striped structure were reproducibly obtained at low-bias voltages ($|V_s| \leq \sim 0.4$ V) with tips sharpened carefully with high-bias-voltage pulses [Figs. 2(a) and

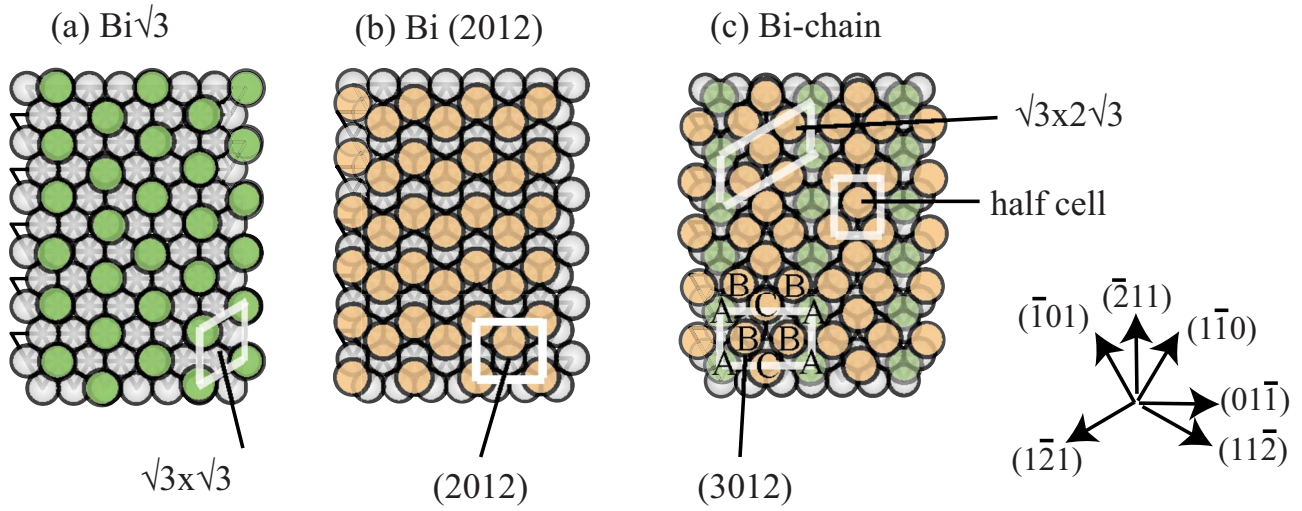

FIG. 3. (Color online) Structural models of the Bi-induced (a) $\sqrt{3}\times\sqrt{3}R30°$, (b) (2012), and (c) (3012) reconstructions. The Ag atoms in the substrates are represented by white circles. On the (a) $\sqrt{3}\times\sqrt{3}$ surface, the Bi atoms in the substitutional sites are represented by green circles. The $\sqrt{3}\times\sqrt{3}$ unit cell is indicated by white lines. On the (b) (2012) surface, the Bi atoms at the threefold sites in the overlayer are represented by orange circles, which are made semitransparent to easily recognize the Bi position on the underlying Ag(111) surface. The (2012) unit cell is shown by white lines. On the (c) (3012) surface, all the Bi atoms are in the overlayer. The Bi atoms at the (a) threefold sites are represented by green circles whereas those at the (b) nearly twofold sites and (c) nearly on-top site are represented by orange circles. The (3012) unit cell is indicated by white lines in the lower left of the structure. For reference, a half unit cell of the (3012) reconstruction and the $\sqrt{3}\times2\sqrt{3}$ unit cell are also indicated.

2(b)]. The arrangement of the protrusions and their contrast were independent of the bias polarity, as demonstrated in the lower right of Fig. 2(b), which indicates that these high-resolution STM images represent the topographic arrangement of atoms at the striped surface structures.

The positions of the protrusions are highlighted by white dots in the high-resolution STM images in Fig. 2, and the size of the dots represents their brightness. The high-resolution STM images show that the atoms are fundamentally arranged with a centered rectangular unit cell [for example, the centered cells on the bright stripes are indicated by white lines in Figs. 2(a) and 2(b)]. However, the contrast of the protrusions is not unique at the surfaces. The contrast of the protrusions is constant along the $\{\bar{2}11\}$ direction but alternates from bright to dark along the $\{01\bar{1}\}$ direction. The alternation of contrast indicates the striped structure extending to the $\{\bar{2}11\}$ direction. The brightest and darkest protrusions have a ~0.01 nm difference in height. The difference in height has no remarkable bias-voltage dependence.

On a more detailed level, the alternation in contrast is not strictly periodic at θ_{Bi}=0.45 ML while it is perfectly periodic at θ_{Bi}=0.75 ML. At θ_{Bi}=0.45 ML, the bright stripes are randomly separated by dark lines with widths of one and two protrusions, as indicated by the white dots and lines in Fig. 2(a) and by the illustration below the STM images in which the bright stripes are displayed as gray lines. The random appearance of the one- and two-protrusion-wide dark lines makes the alternation of the bright and dark stripes aperiodic. Two adjacently centered cells with bright protrusions [highlighted by the white lines in the STM image of Fig. 2(b)] are regularly separated by a dark line with one protrusion width at θ_{Bi}=0.75 ML, as shown in the right and left half of the STM image in Fig. 2(b). The dark line with a width of one protrusion could be regarded as an array of centered rectangular cells with a dark center protrusion along the $\{\bar{2}11\}$ direction. Thus, the periodicity of the stripes could be expressed as an alternation of a centered rectangular cell with bright protrusions (the bright stripe) and one with a dark centered protrusion (the dark stripe). However, an exception was observed in the middle part of Fig. 2(b). Here, the centered cells with the bright protrusions are separated by a dark line with a width of two protrusions. The two-protrusion-wide dark line is regarded as an out-of-phase domain boundary with respect to the periodic alternation of the bright and dark cells in the right and left half of the STM image, where the cells are staggered by a half unit cell length along $\{\bar{2}11\}$, as illustrated by the white dots in Fig. 2(b). Such out-of-phase domain boundaries were observed in other places at θ_{Bi}=0.75 ML. However, the stripe structure was perfectly ordered in each domain at θ_{Bi}=0.75 ML. Therefore, we focus our discussion on the possible surface atomic arrangements for the striped structure in region II for the STM results at θ_{Bi}=0.75 ML.

The first candidate for the striped structure is the (2012) reconstruction. At the Bi/Cu(111) surface, the substitutional Bi-induced $\sqrt{3}\times\sqrt{3}$ reconstruction changes to the (2012) reconstruction at larger coverage.[25] X-ray diffraction (XRD) indicated that the (2012) reconstruction is accompanied by dealloying because further incorporation of Bi atoms into the substitutional sites of the $\sqrt{3}\times\sqrt{3}$ surface alloy layer [Fig. 3(a)] causes the surface stress to become too compressive, and the surface alloy layer becomes energetically unfavorable. The dealloyed Bi atoms assume the threefold hollow sites at the surface and form the (2012) surface reconstruction, as illustrated by the orange circles in Fig. 3(b). The Bi/Cu(111) system is analogous to the Bi/Ag(111) system.

Thus, it can be expected that the Bi/Ag(111) surface also takes the (2012) reconstruction at large θ_{Bi}. The unit-cell size of Ag (0.409 nm) is substantially larger than that of Cu (0.362 nm); therefore, the compressive stress at the Ag(111) surface might be less than that at the Cu(111) surface. However, the atomic radius of Bi(r_{Bi}=0.163 nm) is still larger than that of Ag(r_{Ag}=0.144 nm), and the surface favors the dealloyed structure at larger θ_{Bi}. Thus, Bi atoms are expected to be dealloyed and form the (2012) structure at the Ag(111) surface at $\theta_{Bi} \geq 1/3$ ML.

The (2012) reconstruction has a centered rectangular unit cell, as shown in Fig. 3(b). Furthermore, zigzag-shaped atomic chains [along the horizontal line in Fig. 3(b)] appear periodically. These features resemble those of the striped structure at the Bi/Ag(111) surface. However, the Bi-induced (2012) reconstruction is inconsistent with the striped structure at the Ag(111) surface in terms of the unit-cell size and the direction of the zigzag chains. At the Ag(111) surface, the size of the (2012) unit cell is 2α=0.58 nm in the $\{01\bar{1}\}$ direction and $\sqrt{3}\alpha$=0.50 nm in the $\{\bar{2}11\}$ direction. However, the size of the centered rectangular cell of the striped structure is 0.41 ± 0.01 nm in the $\{01\bar{1}\}$ direction and 0.49 ± 0.01 nm in the $\{\bar{2}11\}$ direction. The difference in the cell size along the $\{01\bar{1}\}$ direction is too large to attribute the striped structure to the (2012) reconstruction. Furthermore, the zigzag chains extend along the $\{01\bar{1}\}$ direction in the (2012) reconstruction whereas the stripes extend along the $\{\bar{2}11\}$ direction at Bi/Ag(111) surfaces.

Alternatively, the stripe structure could be caused by the reconstruction of the Ag(111) surface itself, which includes submonolayer Bi atoms under the surface. However, Bi atoms are essentially immiscible in bulk Ag crystals. From this viewpoint, it is less probable for the stripe structure to be a reconstruction of the Ag(111) surface that includes Bi atoms in the subsurface layers.

As a more realistic model of the periodic stripe structure at θ_{Bi}=0.75 ML [Fig. 2(b)], we propose the surface reconstruction depicted in Fig. 3(c). In this model, all the Bi atoms (represented by green and orange circles) are considered to be dealloyed and adsorbed at sites on the Ag(111) top surface layer. The Bi atom arrangement has the $\begin{pmatrix} 3 & 0 \\ 1 & 2 \end{pmatrix}$ [hereafter, referred to as (3012)] rectangular unit cell, as depicted at the lower left of Fig. 3(c). The (3012) cell is anchored by four corner Bi atoms [the green circles labeled "A" in Fig. 3(c)] at the threefold sites of the Ag(111) surface. XRD studies revealed that the Bi atoms assume threefold sites at the Bi/Cu(111)-(2012) surface.[25] The preference for threefold sites is due to the general trend of Bi to increase the number of coordinated atoms at a surface. Thus, the Bi atoms are also expected to favor the threefold sites and anchor the unit cell of the overlayer Bi atom arrangement at the Ag(111) surface. We then placed Bi atoms (orange circles labeled "B") as hard-touching nearest neighbors to the A Bi atoms at the threefold sites to pack Bi atoms in the unit cell. In this model, in which the sizes of Ag (white circles) and Bi (green and orange circles) atoms are scaled relative to their atomic radii, the B Bi atoms take the *nearly* bridging sites on the two adjacent Ag atoms in the substrate surface. After placing A and B Bi atoms, there is still just sufficient space to place one more Bi atom (orange circles labeled "C") between the four B Bi atoms, as shown in Fig. 3(c). The C Bi atoms are on the nearly on-top site. In the hard-touching ball model, the B and C Bi atoms on the nearly twofold and nearly on-top sites protrude slightly higher along the surface normal direction than the A Bi atoms on the threefold sites. Therefore, it is expected that the orange-colored Bi atoms are imaged brighter than the green-colored Bi atoms in the STM images.

The model agrees with the STM images in Fig. 2(b) in the following respects. The height difference between the protrusions in the bright and dark stripes is ~0.01 nm in the STM images, which is much smaller than the atomic radius of Bi and is reasonably attributed to the corrugation induced by the difference in the adsorption sites. Furthermore, the Bi atoms apparently arrange with the centered rectangular unit cell in the (3012) model [which corresponds to the "half cell" indicated in the right side in Fig. 3(c)]. The contrast of the half cell is periodically alternated along the $\{01\bar{1}\}$ direction. The centered cells with the bright protrusions and those with the dark centered protrusion, periodically alternate along the $\{01\bar{1}\}$ direction. This results in the extension of the bright and dark stripes along the $\{\bar{2}11\}$ direction. The size of the centered cell [marked as half cell in Fig. 3(c)] is one half that of the (3012) unit cell and is ($\sqrt{3}\alpha$=0.50 nm in the $\{\bar{2}11\}$ direction and $3/2\alpha$=0.43 nm in the $\{01\bar{1}\}$) direction. This size is consistent with that of the cell observed in the STM (0.49 nm in the $\{\bar{2}11\}$ direction and 0.41 nm in the $\{01\bar{1}\}$ direction).

The atomic arrangement with the (3012) unit cell could possibly be regarded as having the $\sqrt{3}\times 2\sqrt{3}$ unit cell, as illustrated in Fig. 3(c). Considering the threefold surface rotational symmetry, this would result in a $2\sqrt{3}\times 2\sqrt{3}$ surface diffraction. The $2\sqrt{3}\times 2\sqrt{3}$ reconstruction has been reported as a high coverage phase of the $\sqrt{3}\times\sqrt{3}$ reconstruction at Sb/Ag(111) surfaces at θ_{Sb}=1 ML.[20] Sb, like Bi, is a group V element; therefore, it is reasonable to expect the surface reconstruction of the Sb/Ag(111) system to be similar to that of the Bi/Ag(111) system. Although no model for the atomic arrangement has been reported, the Sb/Ag(111)$2\sqrt{3}\times 2\sqrt{3}$ reconstruction supports the probability of the (3012) model for the stripe structure of the Bi/Ag(111) system.

The (3012) reconstruction model in Fig. 3(c) explains all the features of the high-resolution STM image of the stripe structure [Fig. 2(b)] very well. However, θ_{Bi} of the model is 0.67 ML, which is somewhat smaller than the nominal θ_{Bi} =0.75 ML in Fig. 2(b). We attribute the discrepancy in θ_{Bi} to a partial desorption of Bi atoms during deposition, as was reported for the (2012) phase at the Bi/Cu(111) surface.[25] The Bi atom surface density in the model is very close to that at the surface of the Bi film having a black-phosphorus-like (BP-like) structure. A Bi film with a BP-like structure was recently found to appear at the initial stage of growth on a Si(111)7×7 substrate to lower the surface energy.[36,37] At the surface, the Bi atoms are arranged with a centered unit cell of 0.454×0.475 nm^2. The surface Bi density of the BP-like structure corresponds to θ_{Bi}=0.67 ML at the Ag(111) sur-

face. This surface Bi atom density agrees with that of the model shown in Fig. 3(c). Therefore, the Bi atoms are recognized to be closely packed in the model of the (3012) reconstruction at the Ag(111) surface, as at the surface of the bulk Bi crystal. Additional Bi atoms have weaker adherence to the close-packed Bi layer and are easily desorbed. Thus, the discrepancy in θ_{Bi} between the model and the nominal coverage at the surface prepared at 370–460 K is justified.

Finally, we briefly discuss the striped structure at smaller coverage [i.e., $\theta_{\mathrm{Bi}}=0.45$ ML in Fig. 2(a)]. At smaller θ_{Bi}, the alternation of bright and dark stripes is not strictly periodic due to the random appearance of the one- and two-protrusion-wide dark stripes. This makes the construction of a structural model difficult. However, the Bi atom arrangement still preserves the centered rectangular cell, which suggests a preference for the (3012)-type arrangement. The two-protrusion-wide dark stripes are regarded as out-of-phase boundaries, as in the case of the $\theta_{\mathrm{Bi}}=0.75$ ML surface. At the out-of-phase boundary, two adjacent cells are staggered along the $\{\bar{2}11\}$ direction, and both the right and left side Bi atoms in the two-protrusion-wide dark line take threefold sites to anchor the (3012) unit cell at both sides, as highlighted by the white dots in the middle part of Fig. 2(b). Here, the packing of the Bi atoms in the out-of-phase boundary is looser than that in the (3012) cell. The Bi atoms are not pushed to take the unfavorable nearly twofold and on-top sites, but instead assume the favorable threefold sites in the out-of-phase boundary at the expense of reducing the packing density. The surface density of Bi atoms is less than that of the close-packed value ($\sim$0.67 ML) at $\theta_{\mathrm{Bi}}=0.45$ ML so that the surface introduces out-of-phase boundaries between the (3012) cells at $\theta_{\mathrm{Bi}}=0.45$ ML.

In the end of this section, we discuss the role of the (3012) reconstruction in revealing the origin of the extremely large spin splitting for the Ag(111)$\sqrt{3}\times\sqrt{3}$-Bi reconstruction. The intrinsic Ag and Cu(111) surfaces have *s*-like concave parabolic surface dispersion with $(5s)^1$ and $(4s)^1$ valence electrons, respectively. The Bi atoms with $(6s)^2(6p)^3$ valence electrons change the surface dispersion to be spin-split *p*-like convex parabolas at the $\sqrt{3}\times\sqrt{3}$ surfaces. Theory predicts that the vertical distortion of the surface wave function and the in-plane gradient of the electron potential enhance the splitting of the *p*-like surface dispersions for the $\sqrt{3}\times\sqrt{3}$ reconstruction.[1,6,7,13,18] A recent experimental study revealed that the surface state also has a *p*-like convex dispersion for the Bi/Cu(111)-(2012) surface reconstruction with a large spin splitting.[28] Thus, the large spin splitting of the Bi/Cu-(2022) reconstruction could be attributed to the large vertical distortion in the wave function of the Bi-induced *p*-like surface band caused by the dealloying of Bi atoms. These results suggest that the large spin splitting is characteristic of vertically distorted and in-plane asymmetric *p*-like surface dispersion. In this respect, the Bi-induced (3012) reconstruction at the Ag(111) surface is useful as a touchstone to examine this simple concept. If this is true, dealloying of Bi atoms at the (3012) reconstruction could reveal giant spin splitting, even larger than that at the Bi/Ag(111)-$\sqrt{3}$ surface because the dealloying of Bi enhances the vertical distortion of the wave function for the Bi-induced *p*-like surface-state electrons, more than that for the surface-alloyed Bi-$\sqrt{3}$ reconstruction. Furthermore, the lateral symmetry in the atomic arrangement is broken at every out-of-phase boundary in the Bi/Ag(111)-(3012) reconstruction. Thus, the effect of the in-plane asymmetry and resulting gradient in the lateral potential with large spin splitting could be clarified by comparing the surface dispersion of the low-coverage (3012) reconstruction with many out-of-phase boundaries and that of the high-coverage (3012) reconstruction with almost no out-of-phase boundaries.

IV. SUMMARY

Submonolayer Bi/Ag(111) surface structures were investigated using STM. At $\theta_{\mathrm{Bi}}\leq 1/3$ ML, the Bi atoms occupy substitutional sites and form a surface alloy. Initially, the Bi atoms adsorb randomly, but the $\sqrt{3}\times\sqrt{3}$ ordering increases locally. The $\sqrt{3}\times\sqrt{3}$ reconstruction is completed at $\theta_{\mathrm{Bi}}=1/3$ ML. At larger θ_{Bi}, dealloying occurs and the Bi atoms occupy overlayer sites. The surface structure is then changed to the striped structure. The atomic arrangement in the striped structure is described by the (3012) reconstruction model. The (3012) unit cell is anchored by four corner Bi atoms on the threefold overlayer sites. The other Bi atoms are closely packed on nearly bridging and nearly on-top sites with the same density as that for the BP-like Bi film surface. The difference in the height between the corner and inner atoms causes the contrast of the stripes. In the (3012) reconstruction, the centered half cells with bright centered protrusions and those with dark centered protrusion periodically alternate, which results in the periodic striped structure.

ACKNOWLEDGMENT

This study was financially supported by Grants-in Aid for Scientific Research from the Japanese Society for the Promotion of Science.

*hirayama.h.aa@m.titech.ac.jp

[1] C. R. Ast, J. Henk, A. Ernst, L. Moreschini, M. C. Falub, D. Pacilé, P. Bruno, K. Kern, and M. Grioni, Phys. Rev. Lett. **98**, 186807 (2007).

[2] C. R. Ast, G. Wittich, P. Wahl, R. Vogelgesang, D. Pacilé, M. C. Falub, L. Moreschini, M. Papagno, M. Grioni, and K. Kern, Phys. Rev. B **75**, 201401(R) (2007).

[3] F. Meier, H. Dil, J. Lobo-Checa, L. Patthey, and J. Osterwalder, Phys. Rev. B **77**, 165431 (2008).

[4] K. He, T. Hirahara, T. Okuda, S. Hasegawa, A. Kakizaki, and I. Matsuda, Phys. Rev. Lett. **101**, 107604 (2008).

[5] E. Frantzeskakis, S. Pons, H. Mirhosseini, J. Henk, C. R. Ast,

and M. Grioni, Phys. Rev. Lett. **101**, 196805 (2008).
[6] G. Bihlmayer, S. Blügel, and E. V. Chulkov, Phys. Rev. B **75**, 195414 (2007).
[7] J. Premper, M. Trautmann, J. Henk, and P. Bruno, Phys. Rev. B **76**, 073310 (2007).
[8] F. Reinert, J. Phys.: Condens. Matter **15**, S693 (2003).
[9] Y. A. Bychkov and É. I. Rashba, JETP Lett. **39**, 78 (1984).
[10] S. LaShell, B. A. McDougall, and E. Jensen, Phys. Rev. Lett. **77**, 3419 (1996).
[11] G. Nicolay, F. Reinert, S. Hüfner, and P. Blaha, Phys. Rev. B **65**, 033407 (2001).
[12] M. Hoesch, M. Muntwiler, V. N. Petrov, M. Hengsberger, L. Patthey, M. Shi, M. Falub, T. Greber, and J. Osterwalder, Phys. Rev. B **69**, 241401(R) (2004).
[13] J. Henk, A. Ernst, and P. Bruno, Phys. Rev. B **68**, 165416 (2003).
[14] H. Cercellier, Y. Fagot-Revurat, B. Kierren, F. Reinert, D. Popović, and D. Malterre, Phys. Rev. B **70**, 193412 (2004).
[15] H. Cercellier, C. Didiot, Y. Fagot-Revurat, B. Kierren, L. Moreau, D. Malterre, and F. Reinert, Phys. Rev. B **73**, 195413 (2006).
[16] Y. M. Koroteev, G. Bihlmayer, J. E. Gayone, E. V. Chulkov, S. Blügel, P. M. Echenique, and Ph. Hofmann, Phys. Rev. Lett. **93**, 046403 (2004).
[17] T. Hirahara, K. Miyamoto, I. Matsuda, T. Kadono, A. Kimura, T. Nagao, G. Bihlmayer, E. V. Chulkov, S. Qiao, K. Shimada, H. Namatame, M. Taniguchi, and S. Hasegawa, Phys. Rev. B **76**, 153305 (2007).
[18] L. Moreschini, A. Bendounan, I. Gierz, C. R. Ast, H. Mirhosseini, H. Höchst, K. Kern, J. Henk, A. Ernst, S. Ostanin, F. Reinert, and M. Grioni, Phys. Rev. B **79**, 075424 (2009).
[19] J. Dalmas, H. Oughaddou, C. Léandri, J.-M. Gay, G. Le Gay, G. Tréglia, B. Aufray, O. Bunk, and R. L. Johnson, Phys. Rev. B **72**, 155424 (2005).
[20] P. D. Quinn, D. Brown, D. P. Woodruff, P. Bailey, and T. C. Q. Noakes, Surf. Sci. **511**, 43 (2002).
[21] E. A. Soares, C. Bittencourt, V. B. Nascimento, V. E. de Carvalho, C. M. C. de Castilho, C. F. McConville, A. V. de Carvalho, and D. P. Woodruff, Phys. Rev. B **61**, 13983 (2000).
[22] S. A. de Vries, W. J. Huisman, P. Goedtkindt, M. J. Zwanenburg, S. L. Bennet, and E. Vlieg, Phys. Rev. Lett. **81**, 381 (1998).
[23] D. Pacilé, C. R. Ast, M. Papagno, C. Da Silva, L. Moreschini, M. Falub, A. P. Seitsonen, and M. Grioni, Phys. Rev. B **73**, 245429 (2006).
[24] L. Moreschini, A. Bendounan, H. Bentmann, M. Assig, K. Kern, F. Reinert, J. Henk, C. R. Ast, and M. Grioni, Phys. Rev. B **80**, 035438 (2009).
[25] D. Kaminski, P. Poodt, E. Aret, N. Radenovic, and E. Vlieg, Surf. Sci. **575**, 233 (2005).
[26] R. van Gastel, D. Kaminski, E. Vlieg, and B. Poelsema, Surf. Sci. **603**, 3292 (2009).
[27] C. R. Ast, D. Pacilé, L. Moreschini, M. C. Falub, M. Papagno, K. Kern, M. Grioni, J. Henk, A. Ernst, S. Ostanin, and P. Bruno, Phys. Rev. B **77**, 081407(R) (2008).
[28] S. Mathias, A. Ruffing, F. Deicke, M. Wiesenmayer, I. Sakar, G. Bihlmayer, E. V. Chulkov, Yu. M. Koroteev, P. M. Echenique, M. Bauer, and M. Aeschlimann, Phys. Rev. Lett. **104**, 066802 (2010).
[29] K. Sawa, Y. Aoki, and H. Hirayama, Phys. Rev. Lett. **104**, 016806 (2010).
[30] K. Sawa, Y. Aoki, and H. Hirayama, Phys. Rev. B **80**, 035428 (2009).
[31] M. Miyazaki and H. Hirayama, Surf. Sci. **602**, 276 (2008).
[32] H. Hirayama, Surf. Sci. **603**, 1492 (2009).
[33] G. Neuhold and K. Horn, Phys. Rev. Lett. **78**, 1327 (1997).
[34] F. Silly, M. Pivetta, M. Ternes, F. Patthey, J. P. Pelz, and W.-D. Schneider, Phys. Rev. Lett. **92**, 016101 (2004).
[35] M. Ziegler, J. Kröger, R. Berndt, A. Filinov, and M. Bonitz, Phys. Rev. B **78**, 245427 (2008).
[36] T. Nagao, J. T. Sadowski, M. Saito, S. Yaginuma, Y. Fujikawa, T. Kogure, T. Ohno, Y. Hasegawa, S. Hasegawa, and T. Sakurai, Phys. Rev. Lett. **93**, 105501 (2004).
[37] S. Yaginuma, K. Nagaoka, T. Nagao, G. Bihlmayer, Y. M. Koroteev, E. V. Chulkov, and T. Nakayama, J. Phys. Soc. Jpn. **77**, 014701 (2008).